Summary of Papers Relevant to Capsules

v1

Edgar Häner

17.02.2014

Abstract

Short summaries of papers relevant to experimenting with capsules are given below. The aim of the summary is not completeness but to highlight useful information given in the paper that is not part of the main message, i.e. is not mentioned in the abstract or conclusion. Details of numerical methods used for simulations are not reported.

Contents

1 Making Capsules

1.1 Levy and Edwards-Levy 1996 [1]: Coating alginate beads with cross-linked biopolymers: a novel method based on a transacylation reaction

The authors present a method of creating capsules with membranes using a variety of proteins. The reaction is between a polysaccharides with numerous esterified carboxylic groups and polyamines or proteins, induced by NaHO. This results in the protein directly bound to the acidic polysaccharide. A final neutralization step prevents a further degradation of the film.

The process of making capsules described is as follows:

1. Prepare the initial aqueous solution by dissolving sodium alginate (1 %), a polysaccharidic ester and a protein in distilled water.

   Polysaccharidic ester: 2% propylene glycol alginate (PGA) or 3% pectin

   Protein: 5% human serum albumin (HSA), 8% ovalbumin, 10% hemoglobin or 5% Prosobel

2. Add the resulting solution drop wise to a 10% $CaCl_2$ solution in a ration of 1 to 5 under continued stirring.

3. Rinse beads several times in water.

4. Add NaOH to the suspension of the beads and stir for 15 minutes. Neutralize with HCL and stir for a further 15 minutes.

5. Rinse beads several times in water.

6. Place the coated beads in a 10% solution of sodium citrate solution. Stir for 10 minutes.

7. Rinse beads several times in water.

The proteins HSA and ovalbumin resulted in transparent membranes while hemoglobin and Prosobel resulted in translucent ones. The HSA provided the more solid membranes while ovalbumin ones were thinner and more fragile. While changing the concentration of NaOH changed the membrane thickness with HSA, it did not affect the membrane of ovalbumin.

All proteins result in beads that survive at least a month in water. Note that the capsules swell in water. The swelling increases with decreasing membrane thickness.

1.2 Levy and Edwards-Levy 1999 [2]: Serum albumin alginate coated beads: mechanical properties and stability

They investigate the effect of gelation time, reaction time, NaHO concentration and solvents on human serum albumin alginate coated beads. Specifically, the radius, elasticity, rupture strength and de-formability are measured using a penetrometer. A method to liquefy the core is mentioned.

In general, they found that a salin solution and galation and reaction time of both 5 mins produced optimal results. Specifically, with a concentration of 0.01 NaHO mol/l, the de-formability of the capsules was maximized. Here the membran is much thinner than the core. Higher concentrations of NaHO lead to thicker membranes.

2 Measuring Capsule Properties

2.1 Lardner and Pujara 1980 [3]: Compression of Spherical Cells

The authors develop the theory for the compression of shells with a elastic membrane developed by Feng and Yang [33] for a non-linear elastic material and solve it numerically. The results are compared to earlier compression tests of both rubber balls and sea-urchin eggs and a reasonable agreement is found to the experimental results.

2.2 Carin *et al* 2003 [4]: Compression of Biocompatible Liquid-Filled HSA-Alginate Capsules: Determination of the Membrane Mechanical Properties

An experimental determination of HSA-alginate capsule membrane properties by compression. The capsule is compressed under a known load with one camera (looking down) measuring the contact area and a side-view camera measuring the compression.

Three laws are fitted to the resulting data: a neo-Hookean, the Skalak and the Skalak *et al* laws. The neo-Hookean law was unable to give a constant value of the surface shear elastic modulus G_s over the range of compression tested and hence was found unsuitable to describe membrane properties. Both the Skalak and the Skalak *et al* laws were suitable, giving shear modulus of the same order of magnitude.

2.3 Sherwood *et al* 2003 [5]: Rates of transport through a capsule membrane to attain Donnan equilibrium

Initially, a theory for the passage of salt and water through a membrane that is impermeable to polyelectrolyte molecules is developed. The governing equations predict that the rate at which equilibrium is reached depends only on the external salt concentration.

This is then confirmed using human serum albumin (HSA) - alginate capsules. This allows the measurement of the salt diffusivity of the membrane. This can then be used to infer the Youngs modulus of the capsule membrane given knowledge about the salt diffusivity of the membrane. The governing equation for the radius is

$$r(t) = r - (r - r_0)e^{-k_1 t} \tag{1}$$

where r_0 is the initial radius and r is the final radius. The constant k_1 is

$$k_1 = \frac{3DV_w}{r} \tag{2}$$

where V_ω is the partial molar volume of water (as opposed to anions and cations V_- and V_+) and D is the diffusivity. An estimate of the elastic modulus K can be made by fitting the equation 3 to the experimental data

$$\left(\frac{r}{r_0}\right)^7 - \left(\frac{r}{r_0}\right)^5 = \frac{9}{128\pi^2}\left(\frac{RTV_w}{Kr_0^5}\right)\frac{z_p^2 n_{1p}^2}{x_{2s}} \tag{3}$$

where the symbols are defined in the table below.

An alternative way is to use the initial rate of change of the radius of the capsule, using the estimations for the other values provided in the paper. The initial rate of change of the radius is

$$\left.\frac{\partial r}{\partial t}\right|_{t=0} = -\frac{27DRTz_p^2 n_{1p}^2}{256\pi^2 K r^2 x_{2s}^2}\delta x_{2s} \tag{4}$$

where the symbols are defined as

R	gas constant	T	absolute temperature
z_p	valence of polyelectrolyte ion	n_{1p}	number of moles of polyelectrolyte the inside capsule
x_{2s}	salt mole fraction outside capsule	δx_{2s}	change in salt mole fraction outside capsule

While this theory assumes that the change in salt concentration is small, this is not always true in experiments. Therefore, the mean value for $x_{2s} = \frac{1}{2}(x_{2s}^{initial} + x_{2s}^{final})$ is used.

2.4 Risso and Carin 2004 [6]: Compression of a capsule: Mechanical laws of membranes with negligible bending stiffness

The authors consider three constitutive laws for two dimensional, thin membrans with negligible bending stiffness. The numerical results for the Evans-Skalak (ES), the Mooney-Rivlin (MR) and the Skalak, Tzeren, Zarda, and Chien (STZC) consititive laws are compared to experiments on 8 human serum albumin-alginate capsules. The MR and STZC constituive laws are eliminated.

2.5 Rachik *et al* 2006 [7]: Identification of the elastic properties of an artificial capsule membrane with the compression test: Effect of thickness

The authors consider a compression test of serum albumin-alginate membrane capsules of thickness ratios (h/r) ranging from 2 - 10 %. They compare 3 constitutive laws, each with and without a thin-shell approximation to determine the elastic properties of the capsules. The models investigate were Neo-Hookean, Mooney-Rivlin and the Yeoh model. The capsules were compressed up to 80%.

The thin-shell approximation was only found to be valid for thickness ratios of up to 5%. The Neo-Hookean model was found not to fit the experimental data, while neither the Mooney-Rivlin and the Yeoh model was excluded.

2.6 Risso *et al* 2006 [8]: Experimental investigation of a bioartificial capsule flowing in a narrow tube

A detailed experimental study of millimetric HSA-alginate capsules flowing in a cylindrical tube of $R = 2\,mm$ is conducted. Initially the effect of buoyancy and departure from sphericity are investigated. Buoyancy effects were found to be absent when hydrodynamic forces dominate which happened when the velocity was larger than $5mm/s$ which corresponds to $Ca = \eta_{ext}U/K \sim 0.017$. Similarly, departures from sphericity were negligible when hydrodynamic stresses overcame the initial anisotropic tension.

The behaviour of capsules is best summarized by the authors:

> The evolution of the capsule shape with the capillary number is qualitatively the same for all size ratios. When Ca is increased, the capsule extends in the axial direction and contracts in the radial one. To describe this process in detail, it is useful to distinguish the front, the rear and the intermediate parts of the capsule. During a first stage, the curvature of the front increases and the intermediate part lengthens. When increasing Ca further, both the front and intermediate parts stop evolving. Concerning the capsule rear, initially convex, it first flattens, becomes concave and then becomes more and more concave as Ca is increased.

This is then compared to the literature on numerical simulation. While a general qualitative agreement was found, the exact shape, specifically the rear concave part, did not match.

2.7 Fery and Weinkamer 2007 [9]: Mechanical properties of micro- and nanocapsules: Single-capsule measurements

A review article covering the physics of capsule deformation with reference to all major measurement techniques. The focus is on capsules of micrometre and nanometer size.

2.8 Lefebvre *et al* 2008 [10]: Flow of artificial microcapsules in microfluidic channels: A method for determining the elastic properties of the membrane

An inverse numerical method is developed that allows the inference of capsule membrane properties flowing in a cylindrical tube. This model was developed by Lefebvre and Barthès-Biesel [17]

and is here tested using micrometric ovalbumin-alginate capsules in both cylindrical and square channels.

The values of size ratio $\beta = a/R$ and the flow velocity V are know experimentally. The method of inverse fitting works as follows: a membrane constitutive law (e.g. new-Hookian) is chosen. Initially, the extend of pre-inflation is determined as it can significantly affect the capsule shape is determined. The authors chose $\alpha = 1.5\%$ as this is the smallest level of pre-inflation that gave agreement with experiment.

Then, for given measured values of length in the x-direction L_x/R and length at the centerline L_{fr}/R are used to look up the corresponding value for Ca. As a check, the numerical shape is superimposed over the image of the capsule.

For square channels, the analysis can be adapted. However, as the corners provide space for the fluid to slip past the capsule, smaller deformations of the capsule appear for the same flow rates. This eliminates size rations $\beta < 0.9$ as the deformation is not large enough for accurate determination. Similarly, the approximations used in the theory break down above $\beta > 1.1$.

Note to self: Check A. Diaz and BB 2002, Andry, Edward-Levy and Levy 1996, Queguiner and BB 1997 and Lac and BB 2005

2.9 Hur *et al* 2011 [11]: Deformability-based cell classification and enrichment using inertial microfluidics

The authors demonstrate a microfluidic device that separates rigid particles, liquid drops and cells according to size and deformability. The inertial lift force that creates a force perpendicular to walls is employed to this end. The particle properties, size and elasticity, determine the distance from the wall and hence allows them to be separated. Malignant cancer cells were differentiate from benign cancer cells of the same type, presumably based on their elastic properties.

However, in the demonstration, the cancer cells used were larger than the blood cells. It is unclear whether the elastic properties of the cells play a role in the differentiation. In any case, it is compounded with the absolute size of the cell/particle.

2.10 Chu *et al* 2011 [12]: Comparison between measurements of elasticity and free amino group content of ovalbumin microcapsule membranes: Discrimination of the cross-linking degree

The effect of reaction pH and time on the membrane of micrometric ovalbumin-alginate capsules is tested (different to our capsules), using the inverse numerical method developed by Lefebvre *et all* [10].

The authors find, among other things, that the shear modulus only marginally changes for pH in the range $5 - 7.4$ for short reaction times. However, the shear modulus increases with the reaction time. The inverse nummerical method is more accurate in determining the cross linking degree than the chemical method based on the work of Lévy *et al* [34].

2.11 Chu *et al* 2013 [13]: Automatic Evaluation of the Elastic Modulus of a Capsule Membrane

The authors present an automated numerical method that fits values for the capillary number Ca and the surface shear modulus G_s to experimental data using a neo-Hookean law. Micro-metric ovalbumin-alginate capsules are placed in a circular tube of a radius ($75\ \mu m$) comparable to the capsule radius. The numerical model is based on Lefebvre and Barthès-Biesel [17].

2.12 Hu *et al* 2013 [14]: Characterizing the membrane properties of capsules flowing in a square-section microfluidic channel: Effects of the membrane constitutive law

Ovalbumin microcapsules travelling through a square channel are characterized using the inverse numerical model proposed earlier [22]. Initially, this scenario is investigated with two different constitutive laws, the neo-Hookian and the Skalak *et al* law and different size rations a/l and flow speeds.

At low Ca the shape for both constitutive laws are identical. However, as Ca increases, the neo-Hookian capsule attain parachute shape faster while the Skalak capsules still travel slug shaped. The axis symmetry is broken as the capsules fill the corners.

The experimental pictures are processed using both laws to determine the capillary number Ca. Using the definition $Ca = \mu V/G_s$, the surface shear modulus G_s is extracted as the viscosity μ and the mean velocity of the flow V is known. These ovalbimun capsules are found to be best modelled by a neo-Hookian law as the Skalak *et al* law does not result in a constant value of G_s.

3 Purely Theoretical/Numerical treatments

3.1 Lac and Barthès-Biesel 2005 [15] : Deformation of a capsule in simple shear flow: Effect of membrane prestress

A numerical investigation of uniform prestrees on the behaviour of a spherical capsules suspended in a shear flow. The neo-Hookean and Skalak *et al* laws are used to model the thin hyperelastic membrane. Initially, an analytic model is developed for small deformation. Then numerical simulation are done for large deformation.

They find that a prestress may prevent the buckling instability at low shear shear rates and hence drastically changes the shape of the capsule at a given flow rate.

Note to self: Check Lac, BB, Pelekasis, Tsamopoulos 2004 and BB, Rallison 1981

3.2 Pozrikidis 2005 [16] : Numerical Simulation of Cell Motion in Tube Flow

Abstract:

> A theoretical model is presented for describing the motion of a deformable cell encapsulating a Newtonian fluid and enclosed by an elastic membrane in tube flow. [...] Numerical solutions obtained by a boundary-element method are presented for flow in a cylindrical tube with a circular cross-section, cytoplasm viscosity equal to the ambient fluid viscosity, and cells positioned sufficiently far from the tube wall so that strong lubrication forces do not arise. In the numerical simulations, cells with spherical, oblate ellipsoidal, and biconcave unstressed shapes enclosed by membranes that obey a neo-Hookean constitutive equation are considered. Spherical cells are found to slowly migrate toward the tube centerline at a rate that depends on the mean flow velocity, whereas oblate and biconcave cells are found to develop parachute and slipper-like shapes, respectively, from axisymmetric and more general initial orientations.

3.3 Lefebvre and Barthès-Biesel 2007 [17] : Motion of a capsule in a cylindrical tube: effect of membrane pre-stress

A numerical model for axisymmetric flow of capsules in a cylindrical tube is developed. The thin membrane is modelled using the Mooney-Rivlin, the Skalak *et al* as well as the Evans & Skalak constitutive laws. As recent experiments by Risso *et al* [8] did not correspond to earlier numerical simulations, the effect of membrane pre-stress was investigated. Three inflation ratios, $\alpha = 0, 2.5\%$ and 10% were considered (as in Lac and Barthès-Biesel 2005 [15]).

Two useful parameters to study the shape evolution are $L_x - L_{fr}$, the difference between the total length L_x in the direction of the flow and the length along the centreline or the rear curvature C_r. When measured with the capillary number Ca, it allows a determination of the degree of pre-inflation. L_{fr} follows the same trend as L_x as Ca increases but becomes smaller than L_x when a parachute is formed. $L_x - L_{fr}$ becomes positive at a critical value Ca_c which is relatively sensitive to the degree of pre-inflation. In all cases investigated, the pre-stress decreased the amount of deformation but becomes negligible at high flow-rates.

The results were compared to experimental observations of Risso *et al* [8] and find that the numerical model reproduce the shape observed experimentally for a pre-inflation of 3%. The Skalak *et al* constitutive law is found to best describe the membrane compared to MR and ES laws. The Neo-Hookian law was found inappropriate as it predicts continuous elongation above some critical value of Ca and hence is unsuitable for HSA-alginate capsules.

3.4 Doddi and Bagchi 2008 [18]: Lateral migration of a capsule in a plane Poiseuille flow in a channel

A 3D simulation of capsules with a neo-Hookian membrane in channel with plane Poiseuille flow is studied. In an initial step, the numerical method is validated.

Capillary numbers in the range $0-0.8$ are considered and size ratios a/H in the range $0.1-0.5$. The capsules are started of spherical and off-centre. Initially there is a period of rapid deformation into an ellipsoid shape for moderate flow rates and an asymmetric shape for high flow rates. This is followed by gradual (quasi-static) migration towards the centreline with only slow changes in shape. Larger capsules ($a/H \sim 0.5$) initial shape resembles that of a tear drop with the rounded side pointing towards the centreline.

The effect of an increase in the viscous ratio λ is to lower the migration rate and the deformation of the capsule.

The authors are unaware of experimental migration data for capsules.

3.5 Wolfenden and Blyth 2011 [19]: Motion of a two-dimensional elastic capsule in a branching channel flow

Numerical study of two dimensional Stokes flow of capsules at junctions. Capsules are assumed to have both elastic tension and bending moments and the internal viscosity may differ from the surrounding fluid. A straight channel with a branch coming of at an angle between $\pi/4$ and $3\pi/4$ are investigated. From their conclusion (emphasize mine):

> A capsule inside a branch migrates slowly towards the centreline and relaxes towards an equilibrium shape. It must travel several decades of capsule diameters before the equilibrium shape is fully attained.
>
> For equal flow rates but different daughter widths, capsules will tend to enter the daughter with the highest centreline velocity. When the daughter channels are of equal width and the fluxes are set so that the centreline velocities in the daughters are equal, there is no significant bias towards one or the other. Depending on its line of approach, a capsule may be drawn quickly into the side branch, or it may linger for a considerable time and undergo significant deformation depending on its elastic properties.
>
> In cases where there is no significant directional bias in the capsule motion at the branch junction, the capsule deformation may play a crucial role in determining the ultimate route taken. For stiffer membranes, or when the viscosity inside the capsule is larger than the ambient fluid, the capsule deformation is relatively low. *In some cases, by carefully tuning the elastic membrane stiffness, a capsule following a*

specific line of approach under particular flow conditions can be made to enter the branch or instead to pass over it.

However, a limiting factor is the 2D nature of these calculations as well as the unrealistic large deformation of the capsules.

3.6 Foessel *et al* 2011 [20]: Influence of internal viscosity on the large deformation and buckling of a spherical capsule in a simple shear flow

The authors numerically (3D) investigate the effect of the ratio η of internal to external viscosity. For low viscosity ratios, the internal viscosity do not counteract the capsule deformation. A deformation of $\eta = 0.2$ appears to be representative of all values $\eta \ll 1$ and the deformation is only 10% larger than for $\eta = 1$. Therefore, results obtained for $\eta = 1$ are a first order approximation for all capsules with $\eta \leq 1$

Conversely, large viscosity ratios lower the overall capsule deformation as internal viscous forces balance the compression. Increasing the internal viscosity leads to membrane compression and possibly buckling. Above a critical value of the viscosity ratio η_c, compression zones are found on the capsule membrane for all flow strengths. The critical value depends on the constitutive law and is $\eta_c = 2.5$ for the Skalak and $\eta_c = 1.25$ for neo-Hookean law. Very viscous capsules (i.e. high internal viscosity) tend to buckle easily. The authors note that

> An asymptotic state is reached for highly viscous capsules ($\eta > 5$), with a deformation given by $D_{12} = 5/4\eta$ irrespective of the flow strength and the membrane-constitutive law. Such capsules are expected to exhibit large compression zones, which would be very interesting to study experimentally.

3.7 Kuriakose and Dimitrakopoulos 2011 [21]: Motion of an elastic capsule in a square microfluidic channel

A slightly overinflated capsule made of straining hardening material described by the Skalak *et al* constitutive law is considered (suitable to describe HSA-alginate capsules). The steady state behaviour in a square channel is investigated numerically.

For capsules with a size ratio in the region $0.6 - 0.8$, the shape is deformed into a parachute shape and the cross sectional area decreases (the capsules stretches) as the capillary number increases. In comparison to cylindrical tubes, the behaviour is similar although higher Ca are needed for the square channel to reach the same extend of deformation.

For capsule sizes increases beyond $a/R > 0.9$ the capsule height is restricted by the channel height and the length increases at a larger rate to keep a constant volume. The capsule profile remains symmetric until a size ratio $a/R \sim 0.8$. The evolution of the rear and from curvature and length of capsules with sizes in the range $0.4 \leq a/R \leq 1.3$ are studied in detail. For larger sizes, the pre stress is insufficient to prevent buckling and hence the numerical model diverges.

Scaling laws for various properties are developed for both square and round geometries.

3.8 Hu *et al* 2012 [22]: Flow of a spherical capsule in a pore with circular or square cross-section

The authors develop a 3D model of capsules in a cylindrical tube and compare this with the axis-symmetric model developed earlier. A neo-Hookian constituent law is used. They find good agreement in shape although the 3D model shows oscillation which qualitatively correspond to the compression zones observed in real capsules.

The upper limit Ca_{max} found with the axis-symmetric model by Chu *et al* [12], above which the capsule undergoes continuous extensions, is also found with the 3D model, albeit around 10 % higher. This difference is attributed to the details of the numerical scheme.

For square cross-sections, when $a/l < 1$, there is little difference for low Capillary number Ca but at higher Ca the square capsules tend to be less elongated, as they can expand into the corners, and have a larger cross-section. No buckling occurs in the square capsules. In the case when the capsule is larger than the channel, the square capsule is compressed on the sides and expands into the corners. As the flow increases, the capsule is stretched and the negative tension disappears. At large flow rates, continuous elongation takes over. To attain a similar deformation, the value fo Ca needs to be 60% in the square pore compared to the cylindrical tube.

Using their graphs as a look up table, the authors determine the shear modulus for capsules in a situation similar to that investigated by Lefebvre *et al* [10] and find agreement. No detailed investigation of the accuracy is conducted.

3.9 Park and Dimitrakopoulos 2013 [23]: Transient dynamics of an elastic capsule in a microfluidic constriction

The authors consider a slightly overinflated capsule made of straining hardening material described by the Skalak *et al* constitutive law (suitable to describe HSA-alginate capsules). The behaviour in a square channel with a restriction is investigated, where the height $2l$ of the constriction is half that of the normal channel and the radius a is in the range $0.4 \leq a/l \leq 1$.

The capsule is found to adopt two distinct shapes when entering and leaving the constriction. Initially the front elongates as it enters the constriction and hence the area with a higher flow rate. When it leaves the constriction, the back travels faster than the front leading to an increase in the size perpendicular to the direction of motion and a parachute like shape. Its notable that increasing the size of the capsules is equivalent in effect to decreasing Ca.

The deformation of the capsule decreases with the viscosity ratio of internal to external fluid. A high viscosity ratio also increases the time the capsules takes to return to its steady state in the channel once it left the constriction.

3.10 Kuriakose and Dimitrakopoulos 2013 [24] Deformation of an elastic capsule in a rectangular microfluidic channel

A numerical investigation of lightly overinflated capsule made of straining hardening material described by the Skalak *et al* constitutive law travelling inside a rectangular channel and compare the shapes taken to droplets and vesicles. A channel with an aspect ratio of $l_y/l_z = 2$ is considered.

Capsules with diameters of the order of the smaller dimension of the rectangular channel, at low flow rates, adopt the typical bullet shape also seen in other geometries. As the flow increases, the capsule elongates in the large channel dimension, leading to a pebble shape with a concave back. The authors contrast this to the behaviour of droplets in identical channels.

As the capsule size is increased, the deformation increases. The conclusion of this work is that in rectangular channels, capsule extend in the larger dimension. This is true for varying membrane hardness, pre-stress level and aspect ration, although these can all lead to a more circular shape.

4 Cell / Drop Sorting

4.1 Tan *et al* 2004 [25]: Design of microfluidic channel geometries for the control of droplet volumn, chemical concentration and sorting

4.2 Cartas-Ayala *et al* 2013 [26]: Self-sorting of Deformable Particles in an Asynchronous Logic Microfluidic Circuit

The authors demonstrate a sorting junction that sorts particles based on their hydrodynamic resistance. The main focus of their paper is the differentiation of different gelatin particles (acting as

proxy to cells) but distinguishing of droplets either cured (and hence solid) or liquid (and hence fluid) of equal size is also investigated.

The sorting junction consists of a T-Junction with and additional bypass, exiting the main channel before the junction and joining on of the daughter channels (the Rejection channel). By default the flow in one daughter channel (the Rejection channel) is greater than the other (the Sorting channel) and hence particles will favour the rejection channel. The flow in the bypass is determined by the hydrodynamic resistance of the particle when it is after the bypass bifurcation but still before the T-Junction (the authors call this part of the main channel the Sensing channel). If the particle is large, such that it almost blocks the main channel, a significant portion of the flow will be diverted via the bypass to the rejection channel, reversing the major flow direction at the T-Junction from the Rejection channel to the Sorting Channel.

4.3 Bow *et al* 2011 [27]: A microfabricated deformability-based flow cytometer with application to malaria

A microfluidic device is presented that allows the distinguishing of red blood cells (RBC) based on their deformability in samples of the order $10^3 - 10^4$ cells. The device consists of several (~ 10) consecutive capillary sized constrictions through which the RBC have to deform. Two gemoetries are tested, a convergent, where the entrance is larger and narrows towards the end and a divergent, where the entrance is most constricted and expands afterwards.

This is of particular interest because the parasite causing malaria takes root in the RBC and, by its presence, reduces the deformability of the RBC several fold. This motivates the authors to find a robust, cheap and large sample method of determining the deformability of cells, as that of individual cells rather than a bulk average.

The RBC in a low concentration are inserted into the device and tracked optically as they pass through 10 constrictions and the velocity is measured. To confirm that the deformability of the RCB is the relevant factor, a sample of RCB was altered to reduce the deformability and it was confirmed that with decreasing deformability the average velocity increased. Then, malaria infected RBC with a genetic mutation that makes them fluorescence was used to confirm that these indeed travel slower through the device and are distinguishable by their average velocity.

This experimental observations are further corroborated by a dissipative particle dynamics simulation of the cell deformation as it passes through different constriction geometries.

4.4 Beech *et al* 2012 [28]: Sorting cells by size, shape and deformability

The authors use a Deterministic lateral displacment (DLD) device. This device consists of arrays of posts, in-between which particles smaller than a critical radius R_c move with the flow but larger particles cannot.

This is used for sorting by shape and deformability. By varying the depth of the device, cells (e.g. red blood cell which have side lengths $\sim 7.5\mu m$ and $\sim 2.5\mu m$) are froced into a different orientation, changing their effective Radius to the floe R_{eff}. By measuring the exit position of the cells against the pressure across the device and effective stress-strain graph of the cells is produced.

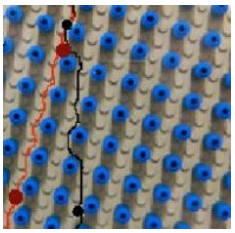

Figure 1: *Schematic of DLD from here*

5 Related

5.1 Link *et al* 2007 [29]: Geometrically Mediated Breakup of Drops in Microfluidic Devices

The authors demonstrate the use of a T-Junction and an obstacle inside a channel as means of breaking up a emulsion of large droplets into a emulsion of small droplets.

5.2 Carlson *et al* 2010 [30]: Droplet dynamics in a bifurcating channel

The authors numerically investigate a droplet hitting a symmetric bifurcation where both daughter channels have equal flow rates. Above a critical Capillary number, the droplet chooses one channel, below this Ca_c it splits into two.

5.3 Kilimnik *et al* 2011 [31]:Inertial migration of deformable capsules in channel flow

Three dimensional computer simulation of rigid and elastic particles in a square channel and their position inside the channel. The authors are mainly concerned with particles that have an aspect ratio $A = d/H < 1/2$ where d is the diameter of the capsule and H is the height of the square channel.

They find that there is monotonic dependence of the equilibrium distance from the centreline and the particle size. Smaller particles travel closer to the wall. Also, this is more pronounced for rigid particles: the more elastic a particle is, the closer to the centreline it will travel for a given size.

5.4 Coupier *et al* 2012 [32]: Shape Diagram of Vesicles in Poiseuille Flow

The authors present a shape diagram of vesicles (bubbles enclosed by lipid bilayer) in Poiseuille flow. These are different from drops or capsules by their inextensible fluid membranes. The investigation is by theory, numerical simulations and experiment and vesicles are classified as bullet, croissant or parachute. Shapes appear to be widest in the narrowest direction of the channel.

References

[1] M.-C. Levy and F. Edwards-Levy, "Coating alginate beads with cross-linked biopolymers: a novel method based on a transacylation reaction," *J. Microencapsulation*, vol. 13, no. 2, pp. 169–183, 1996.

[2] F. Edwards-Lévy and M.-C. Lévy, "Serum albuminalginate coated beads: mechanical properties and stability," *Biomaterials*, vol. 20, pp. 2069–2084, 1999.

[3] T. J. Lardner and P. Pujara, "Compression of spherical cells," *Mech Today*, vol. 5, p. 161176, 1980.

[4] M. Carin, D. Barthès-Biesel, F. Edwards-Lèvy, C. Postel, and D. C. Andrei, "Compression of biocompatible liquid-filled hsa-alginate capsules: Determination of the membrane mechanical properties," *Biotechnol. Bioeng.*, vol. 82, p. 207212, 2003.

[5] J. Sherwood, F. Risso, F. Coll-Paillot, F. Edwards-Lvy, and M.-C. Lvy, "Rates of transport through a capsule membrane to attain donnan equilibrium," *J. Colloid Interface Sci.*, vol. 263, p. 202, 2003.

[6] F. Risso and M. Carin, "Compression of a capsule: Mechanical laws of membranes with negligible bending stiffness," *Phys. Rev. E*, vol. 69, no. 061601, 2004.

[7] M. Rachik, D. Barthes-Biesel, M. Carin, and F. Edwards-Levy, "Identification of the elastic properties of an artificial capsule membrane with the compression test: Effect of thickness," *J. Colloid Interface Sci.*, vol. 301, pp. 217–226, 2006.

[8] F. Risso, F. Collè-Paillot, and M. Zagzoule, "Experimental investigation of a bioartificial capsule flowing in a narrow tube," *J. Fluid Mech.*, vol. 547, p. 149173, 2006.

[9] A. Fery and R. Weinkamer, "Mechanical properties of micro- and nanocapsules: Single-capsule measurements," *Polymer*, vol. 48, pp. 7221–7235, 2007.

[10] Y. Lefebvre, E. Leclerc, D. Barths-Biesel, J. Walter, and F. Edwards-Lvy, "Flow of artificial microcapsules in microfluidic channels: A method for determining the elastic properties of the membrane," *Phys. Fluids*, vol. 20, no. 123102, 2008.

[11] S. C. Hur, N. K. Henderson-MacLennan, E. R. B. McCabec, and D. D. Carlo, "Deformability-based cell classification and enrichment using inertial microfluidics," *Lab Chip*, vol. 11, p. 912, 2011.

[12] T. Chu, A.-V. Salsac, E. Leclerc, D. Barthès-Biesel, H. Wurtz, and F. Edwards-Lvy, "Comparison between measurements of elasticity and free amino group content of ovalbumin microcapsule membranes: Discrimination of the cross-linking degree," *J. Colloid Interface Sci.*, vol. 355, p. 8188, 2011.

[13] T.-X. Chu, A.-V. Salsac, E. Leclerc, and D. Barthès-Biesel, "Automatic evaluation of the elastic modulus of a capsule membrane," in *Knowledge and Systems Engineering* (V.-N. Huynh, T. Denoeux, D. H. Tran, A. C. Le, and S. B. Pham, eds.), vol. 2, pp. 389–398.

[14] X.-Q. Hu, B. Sévénié, A.-V. Salsac, E. Leclerc, and D. Barthès-Biesel, "Characterizing the membrane properties of capsules flowing in a square-section microfluidic channel: Effects of the membrane constitutive law," *Phys. Rev. E*, vol. 87, no. 063008, 2013.

[15] E. Lac and D. Barthès-Biesel, "Deformation of a capsule in simple shear flow: Effect of membrane prestress," *Phys. Fluids*, vol. 17, no. 072105, 2005.

[16] C. Pozrikidis, "Numerical simulation of cell motion in tube flow," *Ann Biomed Eng*, vol. 33, no. 2, p. 165178, 2005.

[17] Y. Lefebvre and D. Barthès-Biesel, "Motion of a capsule in a cylindrical tube: effect of membrane pre-stress," *J. Fluid Mech.*, vol. 589, p. 157181, 2007.

[18] S. K. Doddi and P. Bagchi, "Lateral migration of a capsule in a plane poiseuille flow in a channel," *Int. J. Multiphase Flow*, vol. 34, p. 966986, 2008.

[19] H. C. Woolfenden and M. G. Blyth, "Motion of a two-dimensional elastic capsule in a branching channel flow," *J. Fluid Mech.*, vol. 669, pp. 3–31, 2011.

[20] E. Foessel, J. Walter, A.-V. Salsac, and D. Barthe's-Biesel, "Influence of internal viscosity on the large deformation and buckling of a spherical capsule in a simple shear flow," *J. Fluid Mech.*, vol. 672, pp. 477–486, 2011.

[21] S. Kuriakose and P. Dimitrakopoulos, "Motion of an elastic capsule in a square microfluidic channel," *Phys. Rev. E*, vol. 84, no. 011906, 2011.

[22] X.-Q. Hu, A.-V. Salsac, and D. Barthès-Biesel, "Flow of a spherical capsule in a pore with circular or square cross-section," *J. Fluid Mech.*, vol. 705, pp. 176–194, 2012.

[23] S.-Y. Park and P. Dimitrakopoulos, "Transient dynamics of an elastic capsule in a microfluidic constriction," *Soft Matter*, vol. 9, no. 8844, 2013.

[24] S. Kuriakose and P. Dimitrakopoulos, "Deformation of an elastic capsule in a rectangular microfluidic channel," *Soft Matter*, vol. 9, no. 4284, 2013.

[25] Y.-C. Tan, J. S. Fisher, A. I. Lee, V. Cristini, and A. P. Lee, "Design of microfluidic channel geometries for the control of droplet volumn, chemical concentration and sorting," *Lab Chip*, vol. 4, pp. 292–298, 2004.

[26] M. A. Cartas-Ayala, M. Raafat, and R. Karnik, "Self-sorting of deformable particles in an asynchronous logic microfluidic circuit," *small*, vol. 9, no. 3, pp. 375–381, 2013.

[27] H. Bow, I. V. Pivkin, M. Diez-Silva, S. J. Goldfless, M. Dao, J. C. Niles, S. Suresh, and J. Han, "A microfabricated deformability-based flow cytometer with application to malaria," *Lab Chip*, vol. 11, pp. 1065–1073, 2011.

[28] J. P. Beech, S. H. Holm, K. Adolfsson, and J. O. Tegenfeldt, "Sorting cells by size, shape and deformability," *Lab Chip*, vol. 12, no. 1048, 2012.

[29] D. R. Link, S. L. Anna, D. A. Weitz, and H. A. Stone, "Geometrically mediated breakup of drops in microfluidic devices," *Phys. Rev. Lett.*, vol. 92, no. 5, 2007.

[30] A. Carlson, M. Do-Quang, and G. Amberg, "Droplet dynamics in a bifurcating channel," *Int. J. Multiphase Flow*, vol. 36, 2010.

[31] A. Kilimnik, W. Mao, and A. Alexeev, "Inertial migration of deformable capsules in channel flow," *Phys. Fluids*, vol. 23, no. 123302, 2011.

[32] G. Coupier, A. Farutin, C. Minetti, T. Podgorski, and C. Misbah, "Shape diagram of vesicles in poiseuille flow," *PRL*, vol. 108, no. 178106, 2012.

[33] W. W. Feng and W. H. Yang, "On the contact problem of an inflated spherical nonlinear membrane," *J. Appl. Mech.*, vol. 41, pp. 202–203, 1973.

[34] F. Edwards-Lévy, M. C. Andry, and M.-C. Lévy, "Determination of free amino group content of serum albumin microcapsules using trinitrobenzenesulfonic acid: effect of variations in polycondensation ph," *Int. J. Pharm.*, vol. 96, no. 1-3, p. 8590, 1993.